Journal of Materials Chemistry A

PAPER

View Article Online
View Journal | View Issue

Cite this: J. Mater. Chem. A, 2014, 2, 2383

High-efficiency hybrid solar cells by nanostructural modification in PEDOT:PSS with co-solvent addition†

Joseph Palathinkal Thomas, Liyan Zhao, Donald McGillivray and Kam Tong Leung*

Received 8th November 2013
Accepted 2nd December 2013

DOI: 10.1039/c3ta14590e

www.rsc.org/MaterialsA

Conducting polymer poly(3,4-ethylenedioxythiophene):polystyrenesulfonate (PEDOT:PSS) is gaining technological importance for the fabrication of organic and organic–inorganic heterostructure devices. The conductivity of PEDOT:PSS can be improved by the addition of co-solvents. Here, we show that the simple addition of a suitable wt% of a co-solvent, either ethylene glycol (EG) or dimethyl sulfoxide (DMSO), in PEDOT:PSS can significantly enhance the performance of hybrid solar cells. We provide a morphological model to explain the influence of the co-solvents in PEDOT:PSS, in which the co-solvent modifies the internal crystalline ordering of individual PEDOT nanocrystals that increases the crystal size and forms closely packed nanocrystals, and it also facilitates rearrangement of PSS that reduces its surface chain networks to enhance the polymer conductivity and hybrid solar cell properties. A hybrid solar cell made of EG 7 wt% modified PEDOT:PSS on planar Si exhibits an exceptionally high power conversion efficiency exceeding 12% for the first time.

1. Introduction

Conducting polymers have gained immense interest because of their potential use in low-cost, lightweight, flexible organic semiconductor devices.[1,2] Poly(3,4-ethylenedioxythiophene):polystyrenesulfonate (PEDOT:PSS) is the most studied conducting polymer because of its p-type conductivity, higher light transmittance, and its availability as an aqueous dispersion, which make easy device processability with potential applications in photovoltaic and light-emitting diodes.[2–4] The aqueous dispersion of PEDOT is obtained with the addition of PSS during its synthesis. However, the amount of PSS in PEDOT can influence the electrical properties and may have detrimental effects because of its insulating characteristics. The conductivity of PEDOT:PSS can be improved with the addition of co-solvents.[3–14] Dimethyl sulfoxide (DMSO) and ethylene glycol (EG) have been shown to significantly enhance the electrical properties of PEDOT:PSS in comparison with other co-solvents.[3–9] Recent results from X-ray scattering experiments suggested crystalline ordering of PEDOT nanocrystals with the addition of co-solvents.[5,12] However, their morphological models could not explain the cause for crystal size enhancement. Furthermore, filamentary PEDOT ordering after the addition of a co-solvent in PEDOT:PSS has been observed by Ruit *et al.* by using transmission electron microscopy (TEM).[15] The PEDOT ordering was used to explain the conductivity enhancement, but the observed crystal size reduction after co-solvent addition contradicts earlier reports.[6,10] The latter was clearly due to radiation damage to the soft polymer chains caused by the high-energy electron beam in the TEM, which therefore could not be used to invalidate the PEDOT crystal size enhancement as observed by other groups. Although much effort has been made to investigate the effects of different co-solvents in PEDOT:PSS, most of the studies were conducted on lower conducting grade polymer dispersions. Recently, co-solvent modified PEDOT:PSS (Clevios PH-1000) has been reported to exhibit the highest conductivity (~1000 S cm^{-1}) among the different commercially available varieties of this polymer dispersion.[3,5] The role of the co-solvents in structural modification and size expansion of PEDOT nanocrystals and in their enhancement effects in charge transfer properties of this highly conducting grade polymer dispersion remains an active area of research. Further understanding is important to improve the device performance in applications such as hybrid solar cells.

Recently, PEDOT:PSS has been widely studied for low-cost solar cell fabrication by simply spin-coating the polymer on an n-type Si substrate.[16–21] Solar cell fabrication on planar Si is of great interest because of the cost-effective and less complex fabrication steps, in comparison with the fabrication on structured Si surfaces. It has been suggested that the efficiency of

WATLab and Department of Chemistry, University of Waterloo, Waterloo, Ontario, N2L3G1, Canada. E-mail: tong@uwaterloo.ca

† Electronic supplementary information (ESI) available: Schematic diagram of our hybrid solar cell device structure (Scheme S1), sheet resistance (Fig. S1), and transmittance spectra (Fig. S2) of co-solvent modified PEDOT:PSS films on glass substrates, TOF-SIMS depth profiles (Fig. S3), and Raman (Fig. S4 and S5) and XPS spectra (Fig. S6) of co-solvent modified PEDOT:PSS films. See DOI: 10.1039/c3ta14590e

PEDOT:PSS based solar cells should be comparable to Si-based solar cells, with the theoretical power conversion efficiency (PCE) expected to be about 20%.[22] However, there exists a large range (1–11%) of the achievable PCEs in the literature.[18–25] The variation in PCE can be caused by many factors, including the conductivity of PEDOT:PSS, the amount and/or nature of surfactant used to increase the wettability of PEDOT:PSS on the Si surface, the annealing time and temperature after the spin-coating process, substrate conductivity, interfacial oxide layer thickness, and top and bottom electrode configurations. Better understanding of each of these effects is required to elucidate the causes for the large discrepancy in the PCEs, which ultimately helps to build high-efficiency hybrid solar cells.

Here, we report that the addition of two commonly used co-solvents, DMSO and EG, can significantly change the morphological and nanostructural properties of PEDOT:PSS, and we evaluate their effects on the resulting hybrid solar cell properties. A morphological model is presented to explain the co-solvent-induced modifications of crystalline ordering and size expansion of PEDOT nanocrystals and of the PSS chain rearrangement, which in turn enhance the solar cell properties. We demonstrate an efficiency improvement from 2.4% for a solar cell fabricated on planar Si substrates with PEDOT:PSS (PH-1000) with no co-solvent addition to 12% for a solar cell prepared with 7 wt% EG co-solvent addition, which is the highest efficiency reported to date for this type of solar cells.

2. Experimental

One-side-polished, n-type Si(100) substrates, with a resistivity of 1–10 Ohm cm and a thickness of 200 μm (Virginia Semiconductor Inc.), were ultrasonically cleaned for 10 min successively in acetone, isopropyl alcohol, and Millipore water. After cleaning, the substrates were H-terminated by immersing in 2% hydrofluoric acid for 10 min. Al metal (200 nm thick) was deposited on the unpolished side of the Si substrate in a dual-target magnetron sputtering system (EMS575X) immediately after H-termination. The substrates were allowed to stay in an ambient air atmosphere for 1 h to facilitate the formation of a naturally grown SiO_x layer, because a thin interfacial SiO_x layer could be used to generate a favourable internal electrical field that enhances the solar cell properties.[16,25,26] PEDOT:PSS with a dispersion content of 1.1% in water (Clevios, PH-1000) was mixed with either 3, 5, and 7 wt% DMSO or 3, 5, 7, and 9 wt% EG. To improve the wettability of PEDOT:PSS on Si, 0.25 wt% of a non-ionic surfactant Triton X-100 was also added prior to spin-coating. The PEDOT:PSS layer on Si was coated at a spin rate of 6000 rpm for 1 min and annealed at 110 °C on a hot plate for 10 min in air. For the top electrode, a comb-type Ag metal grid with a thickness of 50 nm was sputter-deposited on the polymer layer through a shadow mask. A schematic diagram of the device structure of the hybrid solar cell is shown in Scheme S1.†

The solar cell properties were analysed using a solar cell characterization system (PV Measurements IV5). The *I–V* measurements were performed under 100 mW cm^{-2} illumination using a class ABA solar simulator (AM 1.5G) in air. The intensity of the light source was calibrated using a Si reference cell (PVM782 with a BK7 window). The measured device area was 6.3 × 6.3 mm^2. The surface morphology and roughness of the samples were examined by tapping-mode atomic force microscopy (AFM) in a Digital Instruments Dimension 3100 Nanoscope IV. Thickness measurements were performed by using reflectometry (Filmetrics F40-UV). Raman spectra were obtained by using a laser with a wavelength of 785 nm (Bruker Senterra) and a laser power of 50 mW. The peak position and accuracy of the instrument were 0.1 cm^{-1} and the resolution was ~3 cm^{-1}. X-ray photoelectron spectroscopy studies were conducted using a Thermo-VG Scientific ESCALab 250 microprobe equipped with a monochromatic Al K_α source (1486.6 eV). Peak fittings for the Raman and XPS spectra were performed by using the Casa XPS software. The PEDOT:PSS before and after co-solvent addition was spin-coated on glass substrates for sheet resistance measurement, which was carried out using the four-point probe method in a van der Pauw configuration (ECOPIA HMS-5300), and for transmittance measurements in the ultra-violet to visible range (Perkin Elmer Lambda-1050). A TOF-SIMS measurement was conducted in an ION-TOF-5 system (IONTOF GmbH), equipped with a 2 m long reflectron time-of-flight analyzer operated in the negative polarity mode, and a Bi_3^+ analysis ion beam source and an Ar cluster ion (Ar_{1000}^+) sputtering beam source. Depth profiling was performed in the spectrometry mode (non-interlaced) with an analysis ion beam current of 0.8 pA, a cycle time of 200 μs, and a sampling area of 150 × 150 μm^2. Sputtering was performed with an Ar cluster ion current of 1.8 nA over an area of 400 × 400 μm^2. The TOF-SIMS spectra were mass-calibrated on C_x fragments.

3. Results and discussion

3.1. PEDOT:PSS-planar Si hybrid solar cell properties

To investigate the influence of co-solvents on the properties of hybrid solar cells, we introduce two different co-solvents, DMSO (3 to 7 wt%) and EG (3 to 9 wt%), into PEDOT:PSS to fabricate hybrid solar cell devices. Fig. 1 shows the current density *vs.* voltage curves for PEDOT:PSS/SiO_x/planar-Si hybrid solar cells before and after the addition of different wt% of DMSO and EG. The respective photovoltaic properties are summarized in Table 1. The solar cell fabricated without co-solvent addition to PEDOT:PSS shows a low PCE of 2.4% despite having a fill factor (FF) of 49% (Fig. 1a). The PCE is found to greatly increase to 11.0% with the addition of 3 wt% DMSO. The PCE decreases slightly to 10.8% and 9.5% for 5 wt% and 7 wt% DMSO additions, respectively. The short-circuit current density, J_{sc}, also increases from 11.4 mA cm^{-2} (no co-solvent) significantly to 27.3, 28.6, and 27.5 mA cm^{-2} for 3, 5, and 7 wt% DMSO additions, respectively. The low open-circuit potential, V_{oc}, increases from 0.43 V (no co-solvent) to 0.56, 0.55 and 0.54 V for 3, 5 and 7 wt% DMSO additions, respectively. A higher FF of 71.6% is obtained for 3 wt% DMSO in comparison to the cells with 5 wt% (68.8%) and 7 wt% (64.8%) DMSO additions. Evidently, the addition of 3 wt% DMSO is remarkably effective in dramatically improving the solar cell properties and higher amounts of 5 and

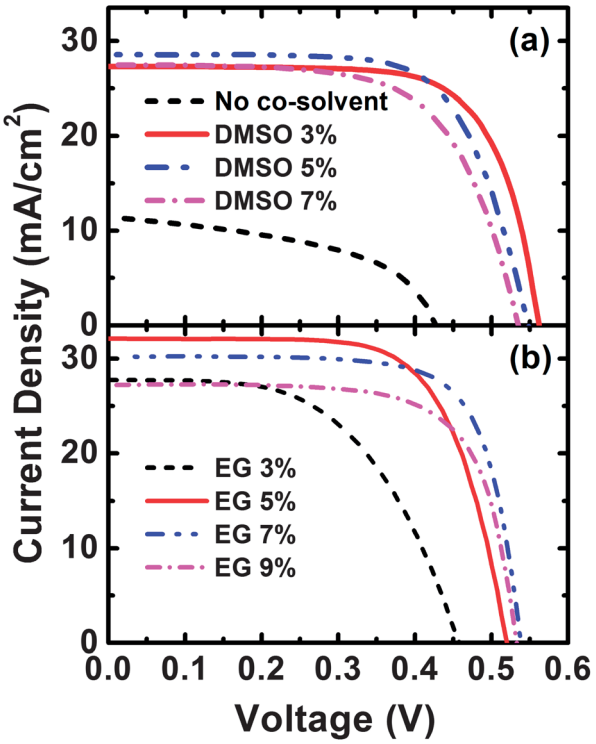

Fig. 1 Current density *vs.* voltage curves of PEDOT:PSS-planar Si solar cells before and after the addition of (a) 3 to 7 wt% DMSO and (b) 3 to 9 wt% EG.

Table 1 Photovoltaic properties of PEDOT:PSS/SiO_x/planar-Si hybrid solar cells before and after the addition of 3 to 7 wt% DMSO and 3 to 9 wt% EG

Co-solvent	J_{SC} [mA cm^{-2}]	V_{OC} [V]	FF [%]	PCE [%]
No co-solvent	11.4	0.43	49.0	2.4
3 wt% DMSO	27.3	0.56	71.6	11.0
5 wt% DMSO	28.6	0.55	68.8	10.8
7 wt% DMSO	27.5	0.54	64.8	9.5
3 wt% EG	27.8	0.46	54.8	7.0
5 wt% EG	32.1	0.52	68.6	11.5
7 wt% EG	30.2	0.54	73.8	12.0
9 wt% EG	27.2	0.53	70.7	10.3

7 wt% DMSO addition slightly reduce the observed improvement. Therefore, further increase in DMSO addition (*e.g.*, 9 wt %) is omitted from this study.

For co-solvent EG, additions of 3 and 5 wt% increase the PCE to 7.0 and 11.5%, respectively, and the PCE reaches an even higher value of 12% with a 7 wt% EG addition (Fig. 1b). The PCE decreases slightly to 10.3% for the cell with 9 wt% EG addition. The J_{sc} also increases from 27.8 (3 wt% EG) to 32.1 mA cm^{-2} (5 wt% EG) and then slightly decreases to 30.2 (7 wt% EG) and 27.2 mA cm^{-2} (9 wt% EG). A higher V_{oc} of 0.54 is achieved for 7 wt% EG, but slightly lower values are found for others (0.46 for 3 wt %, 0.52 for 5 wt%, and 0.53 V for 9 wt% EG). The highest FF of 73.8% is also obtained with the 7 wt% EG addition as compared to the other EG additions of 3 wt% (54.8%), 5 wt% (68.6%), and 9 wt% (70.7%). It should be noted that the variations in the solar cell properties, especially V_{oc} and J_{sc}, are related to the recombination levels in the co-solvent modified PEDOT:PSS and to the front carrier collection efficiency. The PCE of 12% obtained with the 7 wt% EG addition in this work is the highest efficiency ever reported for this type of hybrid solar cells.

Moreover, our sheet resistance (R_s) results show a drastic decrease from 1.3×10^6 Ω sq^{-1} to below 1×10^3 Ω sq^{-1} with the co-solvent addition, except for EG 3 wt% (2.4×10^3 Ω sq^{-1}) (Fig. S1†). The R_s values for the PEDOT:PSS films with 5 and 7 wt % DMSO additions (4.1×10^2 and 2.8×10^2 Ω sq^{-1}, respectively) are lower than that with 3 wt% DMSO addition (9.5×10^2 Ω sq^{-1}), which indicates that even though the conductivity is improved, addition above a certain wt% of DMSO in PEDOT:PSS could lower the solar cell performance. The addition of EG also reduces the R_s considerably to 2.5×10^2 Ω sq^{-1} for EG 5 wt%, and R_s reaches the lowest value of 1.9×10^2 Ω sq^{-1} for the films with 7 and 9 wt% EG additions. On the other hand, the transmittance results show above 85% transmission in the 350–850 nm range for all the samples and the films do not exhibit significant differences in the transmittance properties (Fig. S2†). It is clear that co-solvent addition in PEDOT:PSS does not significantly affect its optical properties, and the related effects do not contribute to the enhancement in solar cell properties. Furthermore, the solar cell properties are evidently in better agreement with the sheet resistance data of the samples with EG addition, which suggests that the carrier transport and collection properties improve with the EG addition in comparison to DMSO addition and these improvements enhance the solar cell performance. In addition, our XPS studies also confirm the reduction in the PSS/PEDOT composition ratio at the surface with increasing amounts of co-solvents in PEDOT:PSS, which affects the sheet resistance, front carrier collection and the solar cell properties.[21,27]

3.2. Structural modifications in PEDOT:PSS due to co-solvent addition

To investigate the influence of co-solvents on surface structure modification in the PEDOT:PSS films, we have carried out AFM studies. Highly smooth surface characteristics for all the solar cell samples are observed. Typical topographic AFM images of PEDOT:PSS films before and after the additions of 3 wt% DMSO and 7 wt% EG are shown in Fig. 2a–c. The AFM image for the PEDOT:PSS without co-solvent addition shows agglomeration of oblate ellipsoidal-shaped PEDOT nanocrystals with individual size ranging from 10 to 25 nm (marked by circles in Fig. 2a). Chain-like nanostructures (marked by arrows in Fig. 2a) at the surface have evidently become obscured after the addition of co-solvents. Furthermore, homogeneous and closely packed PEDOT nanocrystals with enlarged sizes are observed (Fig. 2b and c). By assuming the size of the surface nanostructure is essentially the same as that of the bulk structure, the average PEDOT nanocrystal size, as estimated from the AFM images, appears to increase from 19 ± 6 nm (no co-solvent) to 25 ± 5 nm for 3 wt% DMSO and 30 ± 5 nm for 7 wt% EG additions. For the 7 wt% EG addition, the increase in the PEDOT nanocrystal size

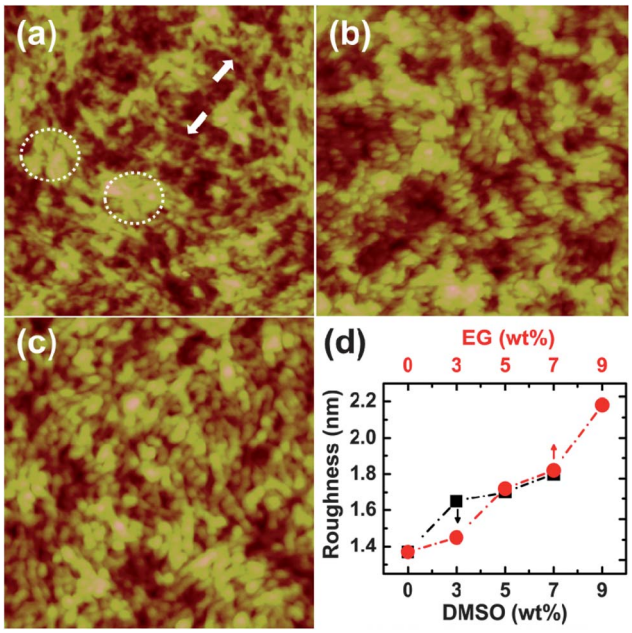

Fig. 2 AFM images (area of 1 × 1 μm^2) of PEDOT:PSS films (a) before and after the addition of (b) 3 wt% DMSO and (c) 7 wt% EG. The circles and arrows in (a) mark the PEDOT clusters and chain-like nanostructures, respectively. (d) Variation in the surface roughness (rms) for the PEDOT:PSS films with the addition of 3 to 7 wt% DMSO (squares) and 3 to 9 wt% EG (circles).

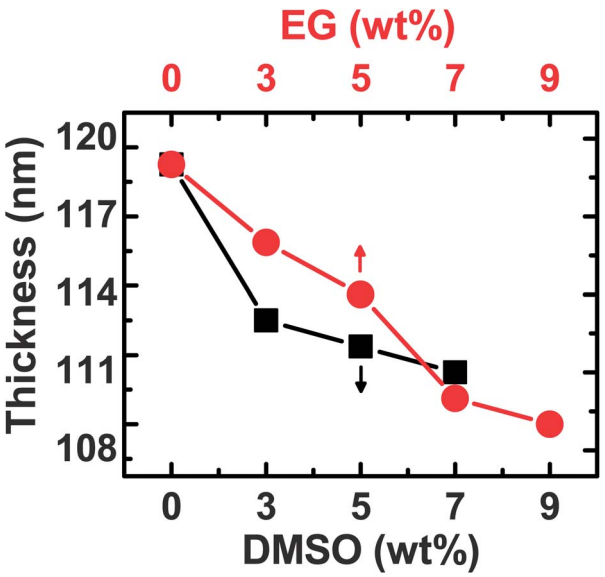

Fig. 3 Variation in the film thickness (estimated by reflectometry) for the PEDOT:PSS films with the addition of 3 to 7 wt% DMSO (squares) and 3 to 9 wt% EG (circles).

enhances the close packing and uniform ordering of PEDOT nanocrystals (Fig. 2c), which promotes charge transfer across the PEDOT:PSS layer and enhances the solar cell properties. In addition to modification of the PEDOT nanocrystal size, slight variations in the surface roughness (rms) and film thickness of PEDOT:PSS films with the addition of co-solvents are also observed. The surface roughness as estimated from the AFM images is plotted in Fig. 2d, while the film thickness (within ±3 nm) as estimated from reflectometry measurement in the range of 200 to 1000 nm is shown in Fig. 3. The surface roughness increases slightly from 1.4 nm for the PEDOT:PSS without any co-solvent to 1.7 nm for 3 and 5 wt% DMSO additions and to 1.8 nm for 7 wt% DMSO addition. For EG addition, the roughness increases more linearly from 1.5 nm for 3 wt% EG to 1.7, 1.8, and 2.2 nm with increasing EG additions of 5, 7, and 9 wt%, respectively. The PEDOT:PSS without any co-solvent shows the highest film thickness of 119 nm. The film thickness is found to reduce to 111–113 nm for 3 to 7 wt% DMSO additions. The film thickness variation shows more linear reduction with the addition of EG, from 116 nm for 3 wt% EG to 114, 110, and 109 nm for 5, 7, and 9 wt% EG, respectively. The change in the thickness is further confirmed by SIMS depth-profiling studies (Fig. S3†), which show similar depth profiles and interface characteristics, where the interface is reached after sputtering for 170 s for the PEDOT:PSS film without any co-solvent as compared to 160 s sputtering for films with 3 wt% DMSO and 7 wt% EG additions. These results indicate that, even after the size enhancement of PEDOT nanocrystals with higher wt% co-solvent addition in PEDOT:PSS, the rearrangement and close-packing of nanocrystals induce slight reduction in the thickness that enhances the conductivity and solar cell properties.

The addition of co-solvents can introduce structural reorganization in PEDOT nanocrystals, which can be evaluated by Raman studies. Most of the major Raman peaks for PEDOT are observed between 1150 and 1610 cm^{-1} (Fig. S4†).[4,8,28–32] Typical Raman spectra for PEDOT:PSS films before and after the additions of 3 wt% DMSO and 7 wt% EG are shown in Fig. 4a. For the Raman spectra of PEDOT:PSS films, the features at 1425 and 1453 cm^{-1} (marked by dashed lines in the figure) correspond to the symmetric stretching modes of C_α–C_β of quinoid and C_α=C_β of benzoid components, respectively, in good accord with the literature.[8,26,28] The peaks observed at 1530 and 1568 cm^{-1} are attributed to the asymmetric C_α–C_β stretching modes. The other discernible peak at 1366 cm^{-1} can be assigned to C_β=C_β stretching vibrations while the features between 1100 and 1300 cm^{-1} correspond to C_α=$C_{\alpha'}$ stretching modes.[8,26] Fig. 4b shows the peak position variations of the two major peaks for the symmetric and asymmetric C_α–C_β stretching vibrations (Fig. S5†). Evidently, except for the sample with the 3 wt% EG addition, the additions of 3 to 5 wt% DMSO and of 5 to 9 wt% EG to PEDOT:PSS cause the symmetric and asymmetric C_α–C_β stretching modes shifted to higher wavenumbers. These shifts can be attributed to the changes in the electronic structure of PEDOT upon oxidation (doping) and rearrangement of the PEDOT chains from the coil-like benzoid structure to a more linear or extended quinoid structure as a result of the co-solvent addition.[4,8,28] The expansion of chains is believed to cause the size increase in the PEDOT nanocrystals observed in the AFM images.

To evaluate the surface properties of the solar cells, we have carried out XPS studies. Typical S 2p spectra of the solar cells before and after the additions of 3 wt% DMSO and 7 wt% EG are shown in Fig. 5a (see also Fig. S6† for XPS spectra of all the

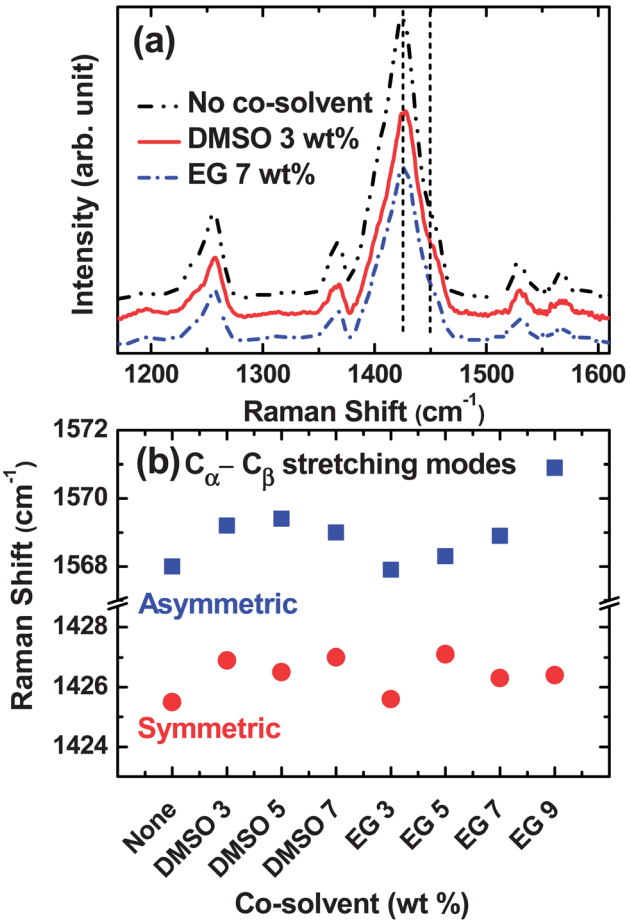

Fig. 4 (a) Raman spectra of PEDOT:PSS films before and after the addition of 3 wt% DMSO and 7 wt% EG. (b) Variation in the Raman shifts for the asymmetric and symmetric C_α–C_β stretch peak positions with the addition of 3 to 7 wt% of DMSO and 3 to 9 wt% of EG.

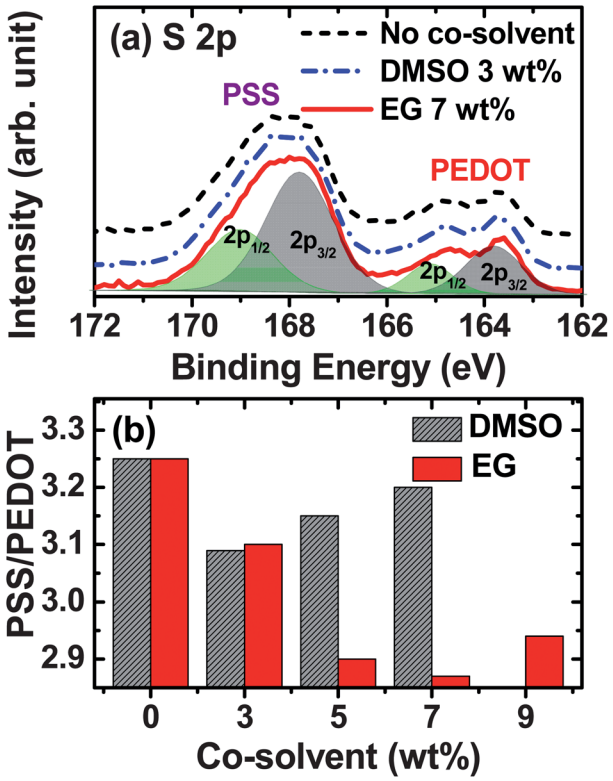

Fig. 5 (a) XPS S 2p spectra of PEDOT:PSS before and after the addition of 3 wt% DMSO and 7 wt% EG. (b) The variation in the ratio of the amount of PSS to that of PEDOT at the surface (as estimated by the ratio of the respective S $2p_{3/2}$ peak areas) with the addition of 3 to 7 wt % DMSO and 3 to 9 wt% EG.

samples). The spectra show two S 2p bands, each corresponding to a doublet of S $2p_{3/2}$ and S $2p_{1/2}$ components with a 1.2 eV spin–orbit splitting and a 2 : 1 intensity ratio. The weaker S $2p_{3/2}$ ($2p_{1/2}$) peak at 163.7 (164.9) eV and the stronger S $2p_{3/2}$ ($2p_{1/2}$) peak at 167.7 (168.9) eV correspond to the sulfur atoms of PEDOT and PSS, respectively.[30] The higher S 2p binding energy found for PSS is due to the electronegative oxygen attachment in the sulfonate moiety. The ratio of the S $2p_{3/2}$ peak areas for PSS and PEDOT can be used to estimate the relative composition of PSS to PEDOT at the surface, and its variation with the addition of co-solvents is summarized in Fig. 5b. The highest PSS/PEDOT surface composition ratio (3.25) is found for the sample without co-solvent addition. The 3 wt% addition of either DMSO or EG reduces the PSS/PEDOT surface composition ratio to 3.10. Increasing the DMSO co-solvent addition to 5 and 7 wt% increases the PSS/PEDOT ratio to 3.15 and 3.20, respectively, while increasing the EG addition to 5 and 7 wt% reduces the PSS/PEDOT ratio to 2.90 and 2.87, respectively. Addition of 9 wt % EG slightly increases the PSS/PEDOT ratio to 2.94. Although the observed variation in the PSS/PEDOT ratio is minimal, it is clear that the highest PCE performance achieved for the solar cell with 7 wt% EG addition is supported by the reduced presence of the PSS chain network at the surface and is in agreement with the observed reduction in the sheet resistance results.

3.3. Mechanism of solar cell property enhancement in PEDOT:PSS due to co-solvent addition

Based on our studies, we propose a morphological model of the PEDOT:PSS films before and after the addition of co-solvents (Scheme 1). In the film without any co-solvent, the oblate ellipsoidal-shaped PEDOT nanocrystals are embedded in the PSS matrix with the PSS chain network largely aligned along the surface. We suggest that the cores of PEDOT nanocrystals are composed of linear chain networks of quinoid components, which is in agreement with the crystalline ordering reported earlier using X-ray scattering studies.[12] These networks are

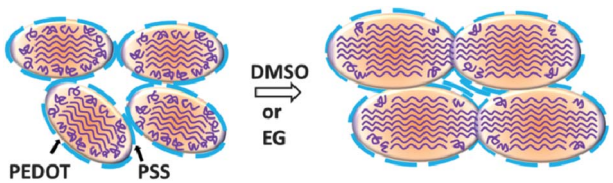

Scheme 1 Schematic model of structural modification in PEDOT:PSS with the addition of co-solvents.

enclosed by randomly oriented coil-like benzoid components near the grain boundary regions. The PEDOT nanocrystals are then surrounded by PSS chains. The higher number of PSS chains on the surface reduces the ohmic contact points to the top electrode along with the less conducting coil-like components at the grain boundaries, which reduces the front surface carrier collection and the efficiency of the solar cell. Addition of a co-solvent enhances the packing density of PEDOT and produces clustering with reduced PSS content at the surface. In addition, the PSS chain network is rearranged to form closely packed domains of PEDOT nanocrystals, which also suppresses defect generation at the interface[25] and results in higher device performance. The increase in the PEDOT nanocrystal size upon addition of the co-solvent suggests an internal re-ordering inside the nanocrystals, which is likely mediated by hydrogen bond formation between the co-solvent and PSS.[4] This co-solvent mediation stabilizes the PSS chains and realigns them along the PEDOT grain boundaries to form intermediate connection with PEDOT nanocrystals. For EG, the polar groups at one end of the EG stabilize PSS, while those at the other end interact with the coil-like polymer chains near the grain boundaries of PEDOT nanocrystals, rearranging them to form a linear and more expanded chain network (*i.e.* changing from a benzoid to quinoid structure). This process is more efficient for EG due to its two polar groups than DMSO with just one polar group.[4] The co-solvent effects appear to saturate after the addition of a sufficient amount of co-solvent (*i.e.* upon reaching a certain wt%). Further addition of co-solvents does not contribute significantly to the internal structural re-ordering of the PEDOT:PSS possibly because of saturation of all the available bonding sites. The highest efficiency obtained from the solar cell with 7 wt% EG addition is attributed mainly to the reordering of a larger number of PEDOT nanocrystals and a reduced amount of PSS chain network on the surface, which enhance the charge transfer across the device structure (from the front electrode to the back electrode) and improve the solar cell performance.

4. Conclusions

A very high solar cell efficiency exceeding 12% for the first time is achieved for PEDOT:PSS-planar Si solar cells with the addition of 7 wt% EG co-solvent. Our study on the effects of addition of co-solvents, EG and DMSO, in a highly conducting grade PEDOT:PSS shows that EG addition is more beneficial to the performance improvement of a PEDOT:PSS based organic–inorganic solar cell. It is important to point out that the extremely high power conversion efficiency reported here is obtained for solar cells fabricated on planar Si, and the present cells are already superior to many solar cells that took advantage of the complex nanostructured Si surfaces reported in recent literature. Our AFM, Raman, and XPS results provide strong evidence for size enhancement and higher ordering of closely packed PEDOT nanocrystals and for reduction in the PSS chain network along the surface, which collectively enhance the solar cell device performance. The present solar cell efficiency could be easily improved by substrate structural modification from planar to pyramidal or nanowire structures.

Acknowledgements

This work was supported by the Natural Sciences and Engineering Research Council of Canada.

Notes and references

1 (*a*) D. N. Congreve, J. Lee, N. J. Thompson, E. Hontz, S. R. Yost, P. D. Reusswig, M. E. Bahlke, S. Reineke, T. V. Voorhis and M. A. Baldo, *Science*, 2013, **340**, 334; (*b*) W. Zhang, B. Zhao, Z. He, X. Zhao, H. Wang, S. Yang, H. Wu and Y. Cao, *Energy Environ. Sci.*, 2013, **6**, 1956.

2 (*a*) D. Alemu, H. Y. Wei, K. C. Ho and C. W. Chu, *Energy Environ. Sci.*, 2012, **5**, 9662; (*b*) Y. Xia, K. Sun and J. Ouyang, *Adv. Mater.*, 2012, **24**, 2436.

3 A. Elschner, S. Kirchmeyer, W. Lovenich, U. Merker and K. Reuter, *PEDOT: Principles and Applications of an Intrinsically Conductive Polymer*, CRC Press, Boca Raoton, FL, USA, 2011.

4 J. Ouyang, C. W. Chu, F. C. Chen, Q. Xu and Y. Yang, *Adv. Funct. Mater.*, 2005, **15**, 203.

5 Q. Wei, M. Mukaida, Y. Naitoh and T. Ishida, *Adv. Mater.*, 2013, **25**, 2831.

6 S. I. Na, G. Wang, S. S. Kim, T. W. Kim, S. H. Oh, B. K. Yu, T. Lee and D. Y. Kim, *J. Mater. Chem.*, 2009, **19**, 9045.

7 S. Ashizawa, R. Horikawa and H. Okuzaki, *Synth. Met.*, 2005, **153**, 5.

8 J. Ouyang, Q. Xu, C. W. Chu, Y. Yang, G. Li and J. Shinar, *Polymer*, 2004, **45**, 8443.

9 J. Y. Kim, J. H. Jung, D. E. Lee and J. Joo, *Synth. Met.*, 2002, **126**, 311.

10 A. M. Nardes, R. A. J. Janssen and M. Kemerink, *Adv. Funct. Mater.*, 2008, **18**, 865.

11 X. Crispin, F. L. E. Jakobsson, A. Crispin, P. C. M. Grim, P. Andersson, A. Volodin, C. V. Haesendonck, M. V. D. Auweraer, W. R. Salaneck and M. Berggren, *Chem. Mater.*, 2006, **18**, 4354.

12 T. Takano, H. Masunaga, A. Fujiwara, H. Okuzaki and T. Sasaki, *Macromolecules*, 2012, **45**, 3859.

13 S. K. M. Jonsson, J. Birgerson, X. Crispin, G. Greczynski, W. Osikowicz, A. W. V. D. Gon, W. R. Salaneck and M. Fahlman, *Synth. Met.*, 2005, **155**, 80.

14 Y. H. Kim, C. Sachse, M. L. Machala, C. May, L. Muller-Meskamp and K. Leo, *Adv. Funct. Mater.*, 2011, **21**, 1076.

15 K. V. D. Ruit, R. I. Cohen, D. Bollen, T. V. Mol, R. Yerushalmi-Rozen, R. A. J. Janssen and M. Kemerink, *Adv. Funct. Mater.*, 2013, **23**, 5778.

16 L. He, C. Jiang, H. Wang, D. Lai and Rusli, *Appl. Phys. Lett.*, 2012, **100**, 073503.

17 H. J. Syu, S. C. Shiu and C. F. Lin, *Sol. Energy Mater. Sol. Cells*, 2012, **98**, 267.

18 B. Ozdemir, M. Kulakci, R. Turan and H. E. Unalan, *Appl. Phys. Lett.*, 2011, **99**, 113510.

19 S. Jeong, E. C. Garnett, S. Wang, Z. Yu, S. Fan, M. L. Brongersma, M. D. McGehee and Y. Cui, *Nano Lett.*, 2012, **12**, 2971.
20 L. He, D. Lai, H. Wang, C. Jiang and Rusli, *Small*, 2012, **8**, 1664.
21 X. Shen, B. Sun, D. Liu and S. Lee, *J. Am. Chem. Soc.*, 2011, **133**, 19408.
22 T. G. Chen, B. Y. Huang, E. C. Chen, P. Yu and H. F. Meng, *Appl. Phys. Lett.*, 2012, **101**, 033301.
23 S. C. Shiu, J. J. Chao, S. C. Hung, C. L. Yeh and C. F. Lin, *Chem. Mater.*, 2010, **22**, 3108.
24 S. Woo, J. H. Jeong, H. K. Lyu, S. Jeong, J. H. Sim, W. H. Kim, Y. S. Han and Y. Kim, *Phys. B*, 2012, **407**, 3059.
25 J. P. Thomas, L. Zhao, M. Abdellah, N. F. Heinig and K. T. Leung, *Anal. Chem.*, 2013, **85**, 6840.
26 F. Zhang, B. Sun, T. Song, X. Zhu and S. Lee, *Chem. Mater.*, 2011, **23**, 2084.
27 C. Y. Huang, D. Y. Wang, C. H. Wang, Y. T. Chen, Y. T. Wang, Y. T. Jiang, Y. J. Yang, C. C. Chen and Y. F. Chen, *ACS Nano*, 2010, **4**, 5849.
28 M. Lapkowski and A. Pron, *Synth. Met.*, 2000, **110**, 79.
29 W. W. Chiu, J. Travas-Sejdic, R. P. Cooney and G. A. Bowmaker, *J. Raman Spectrosc.*, 2006, **37**, 1354.
30 A. Schaarschmidt, A. A. Farah, A. Aby and A. S. Helmy, *J. Phys. Chem. B*, 2009, **113**, 9352.
31 W. W. Chiu, J. Travas-Sejdic, R. P. Cooney and G. A. Bowmaker, *Synth. Met.*, 2005, **155**, 80.
32 S. Garreau, G. Louarn, J. P. Buisson, G. Froyer and S. Lefrant, *Macromolecules*, 1999, **32**, 6807.